High resolution infrared spectroscopy of carbon dioxide clusters up to $(CO_2)_{13}$

J. Norooz Oliaee,[1] M. Dehghany,[1] A. R. W. McKellar,[2] and N. Moazzen-Ahmadi[1]
[1]*Department of Physics and Astronomy, University of Calgary, 2500 University Drive North West, Calgary, Alberta T2N 1N4, Canada*
[2]*Steacie Institute for Molecular Sciences, National Research Council of Canada, Ottawa, Ontario K1A 0R6, Canada*

(Received 13 May 2011; accepted 30 June 2011; published online 28 July 2011)

Thirteen specific infrared bands in the 2350 cm^{-1} region are assigned to carbon dioxide clusters, $(CO_2)_N$, with $N = 6$, 7, 9, 10, 11, 12 and 13. The spectra are observed in direct absorption using a tuneable infrared laser to probe a pulsed supersonic jet expansion of a dilute mixture of CO_2 in He carrier gas. Assignments are aided by cluster structure calculations made using two reliable CO_2 intermolecular potential functions. For $(CO_2)_6$, two highly symmetric isomers are observed, one with S_6 symmetry (probably the more stable form), and the other with S_4 symmetry. $(CO_2)_{13}$ is also symmetric (S_6), but the remaining clusters are asymmetric tops with no symmetry elements. The observed rotational constants tend to be slightly (≈2%) smaller than those from the predicted structures. The bands have increasing vibrational blueshifts with increasing cluster size, similar to those predicted by the resonant dipole-dipole interaction model but significantly larger in magnitude.
 [doi:10.1063/1.3615543]

I. INTRODUCTION

Molecular clusters bound by weak van der Waals forces are of wide interest. In the case of carbon dioxide, the study of clusters has practical importance for atmospheric and even industrial applications, and fundamental importance because of the basic nature of CO_2 itself. More generally, clusters represent the "missing" link between single molecules or molecular pairs and the bulk liquid or solid phases, and intermolecular forces play a key role in this transition region. Carbon dioxide dimers[1–5] and trimers[6–8] were extensively studied by high-resolution infrared spectroscopy in the period from 1984 to 1996. The dimer was shown to have a planar slipped-parallel structure, with centrosymmetric C_{2h} symmetry. Two trimer isomers were identified, one with a planar cyclic structure and C_{3h} symmetry, and the other with a twisted barrel shape and C_2 symmetry. Recent work on CO_2 dimers and trimers has focused on the study of various isotopes,[9,10] and the detection of combination bands[10,11] which provide information on the important intermolecular vibrational modes. All high-resolution work on dimers and trimer has involved either the CO_2 ν_3 antisymmetric stretch fundamental vibration (~2350 cm^{-1}), or the $(\nu_1 + \nu_3)/(2\nu_2 + \nu_3)$ combination vibrations (~3700 cm^{-1}).

There have been many other spectroscopic studies of CO_2 clusters in which rotational structure was not resolved. Dimer features in the $\nu_1/2\nu_2$ Fermi-doublet region (~1300 cm^{-1}) received much attention,[12–17] but have not been very informative, partly because these experiments are performed at relatively high temperatures (>180 K) and gas pressures. Larger clusters have been probed using a number of techniques,[18–27] but $(CO_2)_3$ remained the largest cluster for which explicit infrared band assignments were supported by resolved rotational structure. Very recently, we reported[28] assignments of specific vibration-rotation bands in the ν_3 region to medium-size carbon dioxide clusters, $(CO_2)_N$, with $N = 6$, 7, 9, 10, 11, 12, and 13. These are the largest such clusters to be characterized by rotationally resolved spectroscopy, and the results contribute to bridging the elusive gap between small (dimer, trimer) and large (e.g., microcrystalline[29]) clusters.

The present paper is an expansion and extension of the original brief report.[28] We observe new bands, further investigate the cluster structures, and provide additional details and supporting evidence. Highlights include assignment of a second isomer for the hexamer, $(CO_2)_6$, a combination band for the original hexamer, new redshifted bands for $(CO_2)_{10}$ and $(CO_2)_{13}$, results for ^{18}O-substituted clusters, and a possible alternate structure for $(CO_2)_{10}$.

Intermolecular potential functions for the CO_2–CO_2 interaction have a long history because of its fundamental nature and practical importance. Recent *ab initio* results have utilized SAPT,[30] CCSD(T),[31] and MP2 (Refs. 32 and 33) techniques. Simplified model potential functions which can be quickly evaluated are very useful for molecular simulations, and these may be based on *ab initio* calculations, empirically derived from observed bulk properties, or both.[33–36] An older but noteworthy and widely accepted empirical function is the M-O-M or Murthy potential,[37,38] which was based on solid CO_2 elastic constants but has also been shown to work rather well in predicting dimer and trimer structures, vibrational shifts, and transition moment orientations.[7,8]

II. RESULTS

The apparatus used here has been described previously.[39–42] Spectra were recorded using a rapid-scan tuneable diode laser spectrometer to probe a pulsed

TABLE I. Theoretical binding energies (in cm^{-1}) and theoretical and observed rotational constants (in MHz) for $(CO_2)_N$ clusters.

	M-O-M[a]				SAPT-s[b]				Experiment[c]		
N	Energy	*A*	*B*	*C*	Energy	*A*	*B*	*C*	*A*	*B*	*C*
5	−3405	629.2	421.9	373.6	−3532	630.0	418.4	372.6			
6a	−4664		371.1	295.9	−4886		369.2	298.7		360.1	297.5
6b	−4646		359.6	309.7	−4849		359.1	312.0		352.9	308.7
7	−5891	325.8	272.9	216.8	−6095	322.6	273.9	215.1	314.8	270.7	210.9
8	−7095	297.8	180.4	159.2	−7321	294.2	181.0	158.9			
9	−8456	211.4	163.7	126.8	−8783	210.5	163.9	126.9	207	161	125
10a	−9733	158.8	145.8	110.6	−10 145	158.6	146.4	111.1	155.4	144.0	111
10b	−9778	164.5	145.8	111.3	−10 132	163.4	146.1	111.4			
11	−11 183	138.6	116.1	99.2	−11 644	137.9	116.7	99.8	136	114	106
12	−12 646	111.4	107.7	95.2	−13 191	111.0	108.1	95.8	109	106	93
13	−14 499		94.5	92.8	−15 147		94.8	93.1		92.6	90

[a]Structures from Takeuchi (Ref. 46) based on the empirical potential of Murthyand co-workers (Refs. 37 and 38)
[b]Structures based on the SAPT-s fitted *ab initio* potential of Bukowski *et al.* (Ref. 30)
[c]Present results.

supersonic slit-jet expansion of dilute mixtures of carbon dioxide (∼0.2%) in helium carrier gas. The jet backing pressure was 8 bars and effective cluster rotational temperatures were about 2.5 K. Signals from a fixed etalon and a reference gas cell were used for wavenumber calibration. The PGOPHER program[43] was used for analysis, simulation, and fitting of the spectra. Many of the cluster bands were first observed during searches for CO_2 dimer and trimer combination bands,[10,11] which revealed numerous unexplained features after accounting for known and possible bands of $(CO_2)_2$, $(CO_2)_3$, and CO_2–He.[44,45] In addition to the normal species, some useful cluster results were also obtained using $^{12}C^{18}O_2$, but these were restricted due to limited sample and laser coverage. Earlier $^{13}C^{16}O_2$ spectra[10] had only limited coverage in the dimer and trimer regions and were not of use here.

A. Cluster calculations

Our original assignments[28] were based on calculations of the lowest-energy structures for $(CO_2)_N$ clusters reported by Takeuchi,[46] who used the M-O-M empirical intermolecular potential.[37,38] This function has eight adjustable parameters and consists of atom-atom Lennard-Jones 12-6 terms for the C–C, C–O, and O–O interactions, plus five point charges distributed along the CO_2 axis. Takeuchi reported detailed structural parameters for $N = 4$–40 in his Supporting Information section of Ref. 46 which enabled us to readily calculate the cluster rotational constants, *A*, *B*, and *C*. Subsequently, we made further calculations using the SAPT-s potential, a simplified function based on the high-level *ab initio* results of Bukowski *et al.*[30] These numerical cluster simulations start with *N* molecules in random positions and orientations and adjust the $\{5(N-1)-1\}$-dimensional structure to find an energy minimum for $(CO_2)_N$ using the Powell method from Numerical Recipes.[47] This is repeated hundreds or thousands of times until we are reasonably confident that the true global minimum has been found. This works well for smaller clusters, but the method is crude, compared, for example, to that of Takeuchi,[46] so it becomes impractical for larger clusters (say $N > 14$ in the present case) because of the high dimensionality.

A summary of the results for the minimum energy clusters with $N = 5$–13 using both potential functions is given in Table I. For $N = 6$ and 10, the two lowest energy structures are given. In most cases, the two potentials give very similar results for the structures and rotational constants, with the SAPT-s binding energies generally being about 4% larger. However, our calculation reveals an interesting difference for $N = 10$, where the identities of the two lowest energy isomers interchange between the two potentials. As can be seen in Table I, the lowest energy $(CO_2)_{10}$ isomer using M-O-M, which we label "10b," becomes the second lowest for SAPT-s, and vice-versa for the other isomer labeled "10a." The energy differences are small – only 45 or 13 cm^{-1} in a total binding energy of 10 000 cm^{-1} – so we can still say that the two potentials agree rather well. Although these two $(CO_2)_{10}$ isomers have distinct structures, their rotational constants are similar. As we will see below, isomer 10a seems to agree slightly better with experiment.

The theoretical structures in this range are asymmetric tops ($A > B > C$) except for $N = 6$ and 13, which are oblate symmetric tops ($A = B > C$). But $N = 13$ is very close to the spherical limit, with *B* only slightly larger than *C*. Both the lowest (labeled 6a) and second-lowest (6b) energy isomers of $(CO_2)_6$ are symmetric tops and both have now been observed experimentally (see below). The cluster structures are discussed in more detail below. The special nature of the symmetric ones (especially $(CO_2)_{13}$) is emphasized by the plot of incremental binding energy (or chemical potential) shown in Fig. 1. This is the energy released when cluster *N* is formed by adding a CO_2 monomer to cluster $(N-1)$. Note that $N = 6$ and 13 are local maxima in this plot (also $N = 9$), showing that their structures are especially favorable. Takeuchi shows that $N = 28$ and 40 are also "magic" clusters for CO_2.[46]

Vibrational shifts of molecules in clusters and crystals are frequently modeled using a resonant dipole-dipole model,[8,22,48,49] in which the pairwise interactions of transition dipoles lift the *N*-fold degeneracy of the cluster

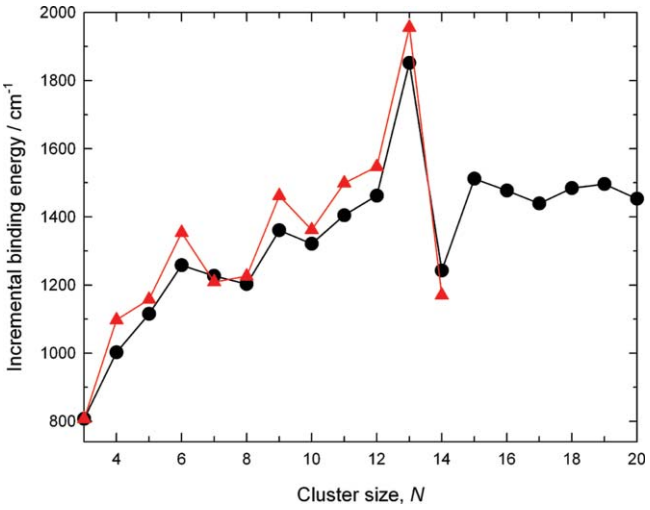

FIG. 1. Incremental binding energy, or chemical potential, for CO_2 clusters, as calculated using the M-O-M (black circles) and SAPT-s (red triangles) intermolecular potentials. Data with $N > 14$ are not given for SAPT-s due to limitations of our structure simulations.

vibrational transition in a way that can be exactly calculated if the structure and transition moments are known. Although this approach should be suitable here because of the large ν_3 dipole transition moment of CO_2, it has actually been shown to be a rather poor model for the CO_2 trimer.[50] But at least it captures the qualitative behavior of CO_2 clusters[28] and represents a useful starting point for discussion. Results of such calculations are shown in Tables II and III. We used an experimental CO_2 transition dipole value[51] (the same as Weida *et al.*[7]) and the SAPT-s structures (M-O-M structures give similar results). For the asymmetric top clusters in Table II ($N = 7$–12), only the three strongest of the N allowed infrared bands are listed. Each band is characterized by its vibrational shift and by the components of its intensity in the directions of the *a*-, *b*-, and *c*-inertial axes. For the symmetric clusters, $N = 6$ and 13 (Table III), all vibrations are listed with their symmetries, vibrational shifts, and intensities.

These resonant dipole results are discussed below in the sections where the various sized clusters are considered in detail. Here we note that there is a general trend for the more intense bands to be blueshifted (positive shifts). Indeed, in Table II there is only one redshifted band, and in Table III a clear majority of the total intensity is blueshifted. This trend for the CO_2 ν_3 mode to blueshift in clusters and condensed phases is experimentally known from previous low-resolution studies.[22,29] It essentially means that excited state cluster binding energies tend to be slightly reduced for stronger bands (i.e., those for which the collective monomer ν_3 vibrations are aligned and in-phase.)

B. The carbon dioxide hexamer, $(CO_2)_6$

The predicted minimum energy structure of the CO_2 hexamer is a symmetric rotor with S_6 point group symmetry (six-fold rotation-reflection axis) as illustrated in at the top of Fig. 2. It can be thought of as a "sandwich" of two cyclic CO_2 trimers with coincident C_3 symmetry axes but with the "top" and "bottom" trimers rotated by 60° with respect to one another. Since all nuclear spins are zero in $^{12}C^{16}O_2$ and $^{12}C^{18}O_2$, the threefold rotation axis implied by S_6 symmetry means that only levels with $K = 3n$ are populated, where n is an integer. As explained in Ref. 28, a band centered around

TABLE II. Summary of resonant dipole calculations for $(CO_2)_N$ clusters.[a]

			Intensity[b]		
N	Shift	Position	*a*	*b*	*c*
7	+0.53	2349.67	0.12	0.96	0.0
7	+4.12	2353.26	1.19	0.05	0.16
7	+5.77	2354.91	0.47	0.09	3.14
8	+1.78	2350.92	1.45	0.67	0.07
8	+5.25	2354.39	0.02	0.17	1.11
8	+6.75	2355.90	1.10	0.03	1.49
9	+1.98	2351.13	2.16	0.11	0.22
9	+3.02	2352.17	0.00	2.19	0.35
9	+4.24	2353.38	0.44	0.00	0.68
10a	−2.07	2347.08	1.61	0.01	0.03
10a	+3.41	2352.55	1.24	0.03	0.03
10a	+10.43	2359.57	0.32	0.44	1.16
10b	+1.19	2350.33	0.05	1.14	0.21
10b	+4.80	2353.94	1.37	0.27	0.88
10b	+6.57	2355.71	0.95	1.01	1.54
11	−3.55	2345.59	0.79	0.51	0.12
11	+3.95	2353.09	0.42	1.48	0.97
11	+10.39	2359.53	0.01	0.89	1.04
12	+3.79	2352.93	0.28	0.44	1.71
12	+4.67	2353.81	0.42	0.43	1.01
12	+12.14	2361.28	1.25	1.04	0.10

[a]Structures calculated from the SAPT-s potential (Ref. 30). Shift and position in cm^{-1}. Only the three strongest bands are given for each cluster size.
[b]Intensities for transition dipole components along the *a*-, *b*-, and *c*-inertial axes, in units of CO_2 monomer transition moment. The total intensity for all bands of cluster $(CO_2)_N$ is equal to N.

TABLE III. Resonant dipole calculation for the two lowest energy isomers of $(CO_2)_6$ and the lowest isomer of $(CO_2)_{13}$.[a]

Isomer	Mode	Shift	Position	Intensity[b]
6a (S_6)	A_u	−3.50	2345.64	0.02
6a (S_6)	E_g	−1.11	2348.03	0.0
6a (S_6)	A_g	+2.00	2351.14	0.0
6a (S_6)	E_u	+1.86	2351.01	5.98
6b (S_4)	E	−3.55	2345.59	0.95
6b (S_4)	E	+1.21	2350.35	4.18
6b (S_4)	B	+2.07	2351.21	0.86
6b (S_4)	A	+2.62	2351.76	0.0
13 (S_6)	A_u	−10.98	2338.16	0.30
13 (S_6)	E_u	−6.15	2342.99	4.10
13 (S_6)	E_g	−4.23	2344.91	0.0
13 (S_6)	A_u	−1.16	2347.98	0.88
13 (S_6)	A_g	−0.16	2348.98	0.0
13 (S_6)	E_g	+1.27	2350.41	0.0
13 (S_6)	A_g	+4.98	2354.12	0.0
13 (S_6)	E_u	+5.47	2354.61	5.80
13 (S_6)	A_u	+14.64	2363.78	1.93

[a]Shift and position in cm^{-1}. Structures calculated from the SAPT-s potential (Ref. 30).
[b]Intensities are in units of CO_2 monomer transition moment, so that the total intensity for all bands of a given cluster is equal to 6 or 13.

TABLE IV. Observed parameters for the S_6 and S_4 isomers of the CO_2 hexamer.[a]

	$(^{12}C^{16}O_2)_6$ S_6 isomer		$(^{12}C^{18}O_2)_6$ S_6 isomer	$(^{12}C^{16}O_2)_6$ S_4 isomer		$(^{12}C^{18}O_2)_6$ S_4 isomer
	Perpendicular fundamental	Parallel combination	Perpendicular fundamental	Perpendicular fundamental	Parallel fundamental	Parallel fundamental
ν_0 / cm^{-1}	2353.5507(1)	2378.1720(1)	2318.5109(1)	2351.8583(1)	2354.4892(1)	2319.4818(1)
B' / MHz	360.114(42)	359.943(45)	328.483(63)	352.731(23)	352.566(19)	322.115(9)
C' / MHz	297.232(24)	297.304[b]	271.355(50)	308.534(46)	308.399(45)	[c]
B'' / MHz	360.141(39)		328.571(61)	352.880(21)		322.367(10)
C'' / MHz	297.505(15)		271.592(52)	308.726(43)		[c]

[a]Centrifugal distortion parameters and the Coriolis zeta parameter for the perpendicular band upper states were fixed at zero.
[b]The quantity $(C'-C'')$ was adjusted to reproduce the observed shape of the Q-branch for the parallel band.
[c]C'' was fixed at 282 MHz for $(^{12}C^{18}O_2)_6$ and $(C'-C'')$ was determined to be −0.025(7) MHz.

2353.55 cm^{-1} (just above "band III" of noncyclic $(CO_2)_3$) (Ref. 8) matches extremely well with that expected from the S_6 hexamer. It is characteristic of a symmetric top perpendicular ($\Delta K = \pm 1$) band for a molecule close to the spherical top limit, and the fitted rotational constants agree very well with the theoretical ones. This 2353.55 cm^{-1} band is shown in Fig. 2 of Ref. 28. The analogous band for the isotopologue $(^{12}C^{18}O_2)_6$ occurs at 2318.51 cm^{-1}.

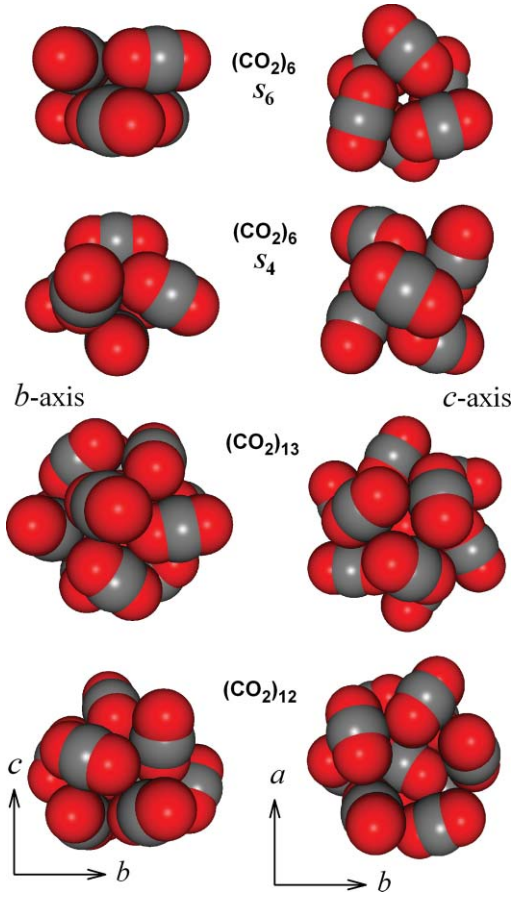

FIG. 2. Illustrations of $(CO_2)_6$, $(CO_2)_{13}$, and $(CO_2)_{12}$. These are "experimental" structures (see text) for $(CO_2)_6$ and theoretical (Ref. 46) ones for $(CO_2)_{13}$ and $(CO_2)_{12}$, but the differences are indistinguishable at this scale. The two lowest-energy isomers of $(CO_2)_6$ have S_6 symmetry and S_4 symmetry as indicated, and the symmetry axis (which is also the c-inertial axis) is out of the plane of the figure in the right-hand views, and in the plane in the left-hand views. $(CO_2)_{13}$ has S_6 symmetry, and the axes are located similarly. $(CO_2)_{12}$ (bottom panel) is an asymmetric top, with inertial axes as indicated.

In addition to this perpendicular band, we have now also observed a weak parallel ($\Delta K = 0$) band at 2378.17 cm^{-1} for which the fitted B-value is virtually identical (as usual for a symmetric top parallel band the C-value was not well determined). The corresponding parallel band was not observed for $(^{12}C^{18}O_2)_6$ due to limited laser coverage. For our analysis, we assumed that the perpendicular and parallel bands arise from the same ground state and performed a simultaneous fit with results as shown in Table IV. Coriolis coupling in the upper state of the perpendicular band was neglected, an approximation which is reasonable, based on the general observation that intramolecular vibrations are only loosely coupled in weakly bound complexes and on the rather similar case of the cyclic CO_2 trimer.[7] Most fitted lines in the analyses represent blends of numerous individual transitions, and there are many overlapping features from other CO_2 clusters, particularly for the perpendicular bands. For these reasons, the statistical errors in Table IV probably underestimate the true parameter uncertainties.

With the assumption of S_6 symmetry, the hexamer has four fundamental vibrational modes in the CO_2 ν_3 region (see Table III). There is an infrared-forbidden mode with A_g symmetry, corresponding to in-phase ν_3 vibrations on all six monomers. There is a mode with A_u symmetry in which the "upper" three monomers vibrate in-phase, and the "lower" three also vibrate in phase, but with the two sets out-of-phase. Although this A_u mode gives rise to an allowed c-type band, it is very weak because the monomers have little projection on the c axis (the individual trimer units within the hexamer are almost planar). There are two degenerate modes, a forbidden one with E_g symmetry, and an allowed one with E_u symmetry. It is the latter E_u mode which gives rise to a strong perpendicular band to which we assign the observed bands at 2353.55 and 2318.51 cm^{-1}. The parallel band at 2378.17 cm^{-1} could be due to the A_u fundamental, but because of its large blueshift we believe it is really a combination band involving the sum of an intramolecular fundamental plus a low-frequency intermolecular mode. The most likely intermolecular modes are those in which the trimer units within the hexamer execute out-of-plane "torsional" motions because these are just the modes that have been observed for the cyclic trimer itself.[10,11] In the trimer,

these modes have frequencies of about 13 and 19 cm^{-1}. In the hexamer, this mode has a frequency of 25.62 cm^{-1} if the associated fundamental is the E_u one observed here (in which case the intermolecular mode would be E_g). But we cannot be sure of this because an upper state with the required A_u symmetry can also be generated by combining any one of the four intramolecular fundamentals with an intermolecular mode of the appropriate symmetry. What is clear is that the unambiguous observation[10,11] of parallel combination bands for cyclic $(CO_2)_3$ makes the observation of an analogous band of $(CO_2)_6$ very plausible, since the hexamer is essentially composed of two trimers.

The observed vibrational shifts of the hexamer fundamental band origins with respect to the CO_2 monomer are +4.408 and +4.462 cm^{-1} for $(^{12}C^{16}O_2)_6$ and $(^{12}C^{18}O_2)_6$, respectively. These are in the same direction, but considerably larger than the shift of +1.86 cm^{-1} predicted by the resonant dipole model (Table III). The two experimental rotational constants determined for $(^{12}C^{16}O_2)_6$ are not sufficient to determine its structure completely, and the $(^{12}C^{18}O_2)_6$ data do not give much additional information. To estimate an experimental structure, we make the following assumptions: the monomer geometry remains unchanged in the hexamer; each trimer unit remains planar in the hexamer; and the in-plane orientation angle of the monomer in the trimer is $\beta = 40°$.[7,50] With these restrictions, the observed $(^{12}C^{16}O_2)_6$ constants give values of 2.897 Å for the distance between the two trimer planes, and 4.045 Å for the C–C distances within each trimer unit. For comparison, some values for these distances from theoretical potential surfaces are 2.813, 2.773, and 2.897 Å and 4.036, 4.060, and 4.064 Å.[30,46,52] The experimental C–C distance for the trimer is 4.030 Å.[7] However, note that the theoretical structures have slightly nonplanar trimer units in the hexamer, whereas we assume they are planar. Our "experimental" hexamer structure predicts isotope shifts of −31.02 and −26.14 MHz for B'' and C'' between $(^{12}C^{18}O_2)_6$ and $(^{12}C^{16}O_2)_6$, in good agreement with the observed values of −31.57 and −25.91 MHz.

C. Another isomer of the hexamer

The next lowest energy isomer of $(CO_2)_6$ is predicted to lie only 18 (M-O-M) or 36 cm^{-1} (SAPT-s) higher in energy. It is also a symmetric top, but this time with S_4 symmetry. As illustrated in Fig. 2, it consists of a ring of four equivalent monomers capped at the "top" and "bottom" by a pair of equivalent monomers. These two monomers are aligned orthogonally, so that by themselves they would have D_{2d} symmetry. The ring of four monomers is slightly puckered, meaning that the four equivalent C atoms are not (necessarily) planar. According to Liu and Jordan,[53] the M-O-M potential predicts an interconversion barrier of about 1 kcal/mol (350 cm^{-1}) between isomers 6a and 6b.

We assign two bands to this form of the hexamer. There is a parallel band, already reported but unexplained,[10] with a Q-branch at 2354.49 cm^{-1}, a clear R-branch, and a heavily obscured P-branch. Its analysis gave $B'' = 351$ MHz, about 8 MHz smaller than the calculated value for isomer 6b in Table I. Note that the observed B'' for isomer 6a is similarly about 10 MHz smaller than the calculated values. There is also a perpendicular band centered at 2351.86 cm^{-1} having a Q-branch similar to that of the original hexamer at 2353.55 cm^{-1}, but with narrower line spacing. This spacing (≈180 MHz) is close to that predicted (188 MHz) for the S_4 hexamer (this predicted value is equal to $2\times2\times(B-C)$, where one factor of 2 comes from the fact that only levels with $K = 2n$ are populated due to spin statistics and the twofold rotation axis implied by S_4 symmetry). These bands are illustrated in Fig. 3. The perpendicular one is heavily overlapped by transitions of $(CO_2)_2$ and $(CO_2)_3$, the latter including both the cyclic trimer and band III of the noncyclic trimer. As well, there is interference from other unassigned transitions, including the P-branch of the so-called Q_A band (which may be due to $(CO_2)_4$).[7,8,10] In spite of this interference, we were able to assign a reasonable number of perpendicular band transitions and perform a simultaneous analysis of both bands, yielding the parameters listed on the right-hand side of Table IV. This gave values of B'' and C'' in good agreement with theory (see Table I). For $^{12}C^{18}O_2$, we observed the analogous parallel band at 2319.48 cm^{-1} (see Table IV), but missed the perpendicular band due to limited laser coverage.

The S_4 hexamer has four fundamental modes in the CO_2 ν_3 region (see Table III). There are two degenerate vibrations

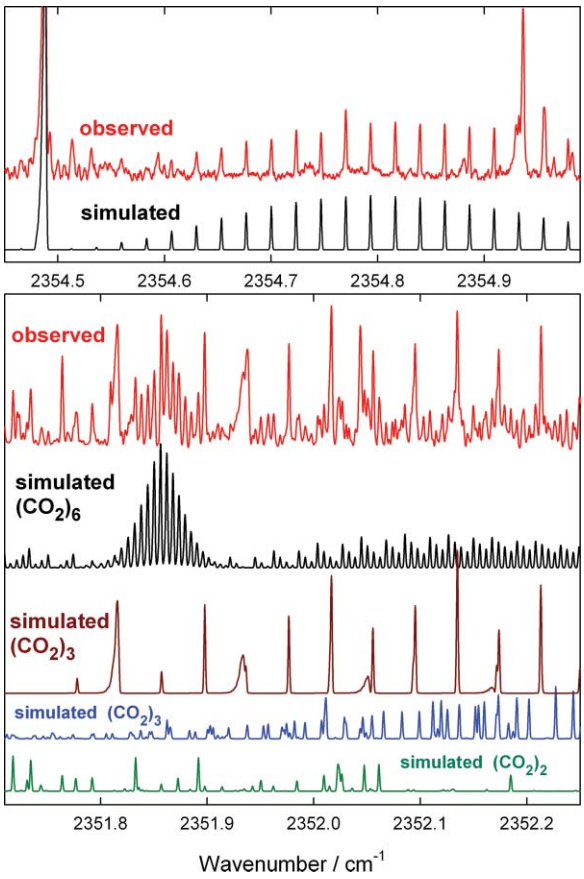

FIG. 3. Observed and simulated spectra showing bands assigned to the S_4 isomer of $(CO_2)_6$. The perpendicular band in the lower panel is overlapped by bands of $(CO_2)_2$ and of the cyclic (brown) and noncyclic (blue) isomers of $(CO_2)_3$ as shown, while the Q- and R-branches of the parallel band in the upper panel are relatively clear.

with E symmetry giving rise to perpendicular bands, a vibration with B symmetry giving rise to a parallel band, and a vibration with A symmetry which is infrared forbidden. According to the resonant dipole calculation in Table III, we expect a redshifted (-3.5 cm^{-1}) perpendicular band, a much stronger blue-shifted ($+2.1$ cm^{-1}) perpendicular band, and a more blueshifted ($+2.6$ cm^{-1}) parallel band. The observed perpendicular and parallel bands, with shifts of $+2.72$ and $+5.35$ cm^{-1}, respectively, are indeed blueshifted, but, as usual,[28] these shifts are considerably larger in magnitude than predicted by the simple model. Since another perpendicular band is predicted, we checked carefully and found a possible candidate Q-branch at about 2348.33 cm^1 (a vibrational shift of -0.81 cm^{-1}). However, this band was too weak to analyze in detail.

Assuming S_4 symmetry and unchanged monomers, three distances and three angles are required to specify the structure of isomer 6b, and these can be expressed as follows. First, the "ring radius" distance from the S_4 symmetry axis to one of the four equivalent C atoms. Second, the "hexamer length" distance between the two equivalent C atoms. Third, the "ring puckering" distance from the center of mass to the line connecting diagonally opposite pairs of the four equivalent C atoms (in the SAPT-s structure, this distance is 0.075 Å – if it is zero then the four equivalent C atoms are coplanar). Then there is the angle between the O–C–O axis of one of the two equivalent monomers and one of the lines connecting diagonally opposite pairs of the four equivalent C atoms (since each subunit is a symmetric top, this angle has no effect on the hexamer rotational constants – it is like internal rotation in ethane). More significant is the angle between the O–C–O axis of one of the four equivalent monomers and the line connecting its C atom with the diagonally opposite C atom. Finally, there is the dihedral angle between the O–C–O axis of one of the four equivalent monomers and the S_4 symmetry axis. With six unknowns and only two observables (or three, counting the $(^{12}C^{18}O_2)_6$ B-value), it is not possible to determine the structure experimentally. However, for illustration we keep all angles and the puckering distance fixed at the SAPT-s values and vary the two remaining distances to fit B'' and C'' of the normal isotopologue. By changing the "ring radius" from 2.818 (SAPT-s) to 2.836 Å, we obtain the experimental C'' value. Then by changing the "hexamer length" from 5.043 (SAPT-s) to 5.115 Å, we get the experimental B''-value. The isotope shift for B'' predicted by this "experimental" structure agrees perfectly with experiment.

D. The carbon dioxide heptamer (or septamer), $(CO_2)_7$

We assign bands at 2356.25 and 2321.14 cm^{-1} to $(^{12}C^{16}O_2)_7$ and $(^{12}C^{18}O_2)_7$, respectively.[28] They are (mostly) c-type bands with prominent Q-branches and extensive P- and R-branch structure, as illustrated in Fig. 4. The detailed match between observed and simulated spectra is very good. The fitted rotational constants (Table V) agree quite well with predicted ones (Table I), and this agreement is somewhat better for $(^{12}C^{18}O_2)_7$ than for $(^{12}C^{16}O_2)_7$ (rms deviations of 4.4 vs. 5.4 MHz for the SAPT-s structure) as expected if part

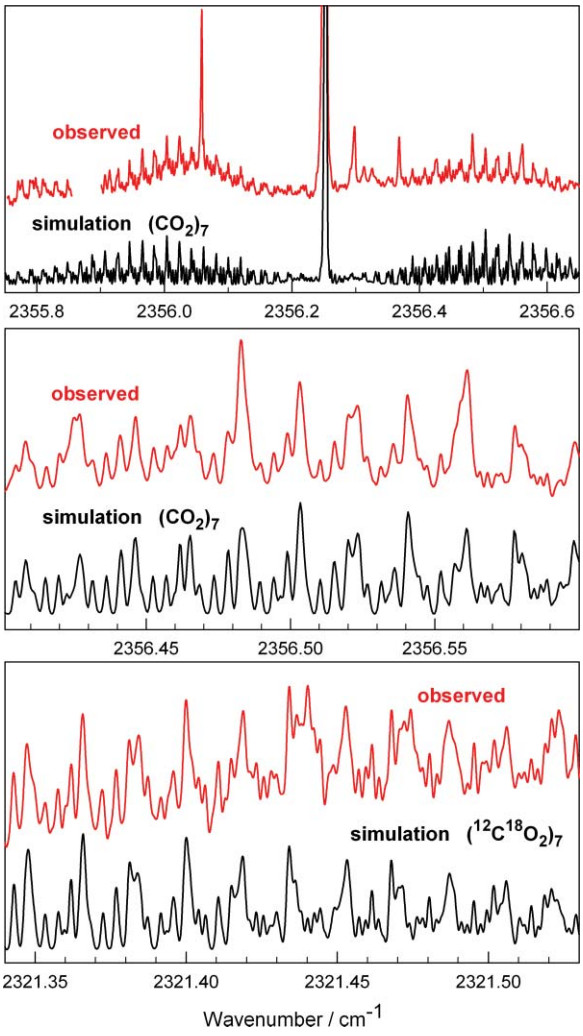

FIG. 4. Observed and simulated spectra showing bands assigned to $(CO_2)_7$. The top panel is an overview of the entire $(^{12}C^{16}O_2)_7$ band. The middle and bottom panels show detailed views of the R-branch for $(^{12}C^{16}O_2)_7$ and $(^{12}C^{18}O_2)_7$, respectively.

of the discrepancy is due to zero-point motion effects. There is a hint of some b-type contribution to the bands (at most 0.3 of the c-type), but not of any a-type transitions (<0.2).

The predicted heptamer structure is unsymmetrical, with five monomers in a pentagonal ring approximately in the plane of the a- and b-inertial axes and the remaining two located close to the c axis above and below the ring. In the absence of help from symmetry, there is no way to refine

TABLE V. Observed parameters for $(CO_2)_7$.[a]

	$(^{12}C^{16}O_2)_7$	$(^{12}C^{18}O_2)_7$
ν_0 / cm^{-1}	2356.2545(1)	2321.1378(1)
A' / MHz	314.636(42)	287.895(88)
B' / MHz	270.531(46)	247.784(71)
C' / MHz	210.720(340)	193.525(397)
A'' / MHz	314.809(45)	288.110(98)
B'' / MHz	270.726(49)	247.324(96)
C'' / MHz	210.860(242)	193.618(395)

[a]Centrifugal distortion parameters were fixed at zero. The parameters are slightly different from those reported previously (Ref. 28) because the fit has been refined.

the theoretical structure using the experimental rotational constants. The results do at least provide a benchmark for future high-level calculations of the heptamer structure. Since there are no equivalent monomers, there should be seven infrared-allowed fundamentals in the ν_3 region of which we have observed one, with a vibrational shift relative to the CO_2 monomer of +7.11 or +7.09 cm^{-1} for $(^{12}C^{16}O_2)_7$ or $(^{12}C^{18}O_2)_7$, respectively. The resonant dipole model (Table II) predicts the strongest band to be mostly *c*-type and shifted by +5.77 cm^{-1}, in reasonable qualitative agreement with experiment. The next lowest energy isomer of $(CO_2)_7$ predicted by the SAPT-s potential is about 56 cm^{-1} higher in energy and is also unsymmetrical, with rotational constants $(A, B, C) = 302.9, 276.2, 193.6$ MHz.

E. The carbon dioxide nonamer $(CO_2)_9$ and decamer $(CO_2)_{10}$

The band at 2358.69 cm^{-1} which we assign to $(CO_2)_9$ has a strong sharp *Q*-branch with rather weak and indistinct *P*- and *R*-branches, as shown in the top trace of Fig. 5. There is regular *P*- and *R*-structure with a spacing corresponding to an effective rotational constant of about 180 MHz. From the theoretical rotational constants (Table I), this spacing could be given either by an *a*-type band of $(CO_2)_8$ (predicted $(B + C)/2 \approx 170$ MHz), or by a *c*-type band of $(CO_2)_9$ (predicted $(A + B)/2 \approx 188$ MHz). A simulation based on $(CO_2)_8$ gives structure much more pronounced than observed ($(CO_2)_8$ is relatively close to the prolate symmetric limit). A simulation with constants close to those predicted for $(CO_2)_9$, shown in the top panel of Fig. 5, is much better. The corresponding $(^{12}C^{18}O_2)_9$ band may be located at 2323.669 cm^{-1}, but is less clear. It would represent a shift of +9.62 cm^{-1} from the monomer origin, as compared to +9.54 cm^{-1} for the normal isotope. The predicted structure of $(CO_2)_9$ is unsymmetric, with nine allowed bands in the ν_3 region of which the resonant dipole model predicts the third strongest to be predominantly *c*-type with a shift of +4.24 cm^{-1}. We are reasonably sure that $(CO_2)_9$ provides the correct assignment for this band, but the simulation is not perfect and this is one of our less secure identifications, together with $(CO_2)_{11}$ (below).

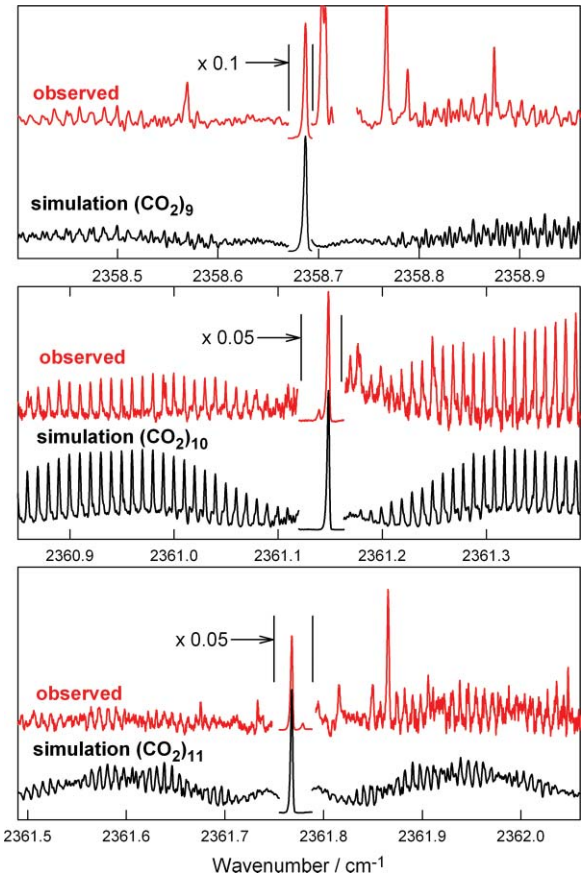

FIG. 5. Observed and simulated CO_2 cluster spectra showing bands assigned to $(CO_2)_9$, $(CO_2)_{10}$, and $(CO_2)_{11}$. The signals in the regions around the strong central *Q*-branches are multiplied by factors of 0.05 or 0.10 as indicated.

We observe a strong, sharp *Q*-branch at 2361.15 cm^{-1}, which is accompanied by long and regular series of *P*- and *R*-branch lines (middle panel of Fig. 5). A good simulation of the band is obtained using constants (Table VI) close to those predicted for $(CO_2)_{10}$. The simulation is a *c*-type band with a weaker *a*-type contribution (intensity ratio $a{:}c = 1{:}4$). This band is not sensitive to the absolute value of *C*, so the fitted value (111 MHz) is only approximate. Nevertheless, the good agreement with the predicted *A* and *B* values for $(CO_2)_{10}$ is strong support for the present assignment, compared to any other cluster size. A similar but much weaker band (not shown here) was observed at 2344.08 cm^{-1} whose shape was consistent with assignment as another *c*-type band of the same species. There is a corresponding band for $(^{12}C^{18}O_2)_{10}$ centered at 2326.109 cm^{-1}, but its *P* and *R* structures are barely evident so we cannot confirm the assignment. This would represent a shift of +12.06 cm^{-1} from the monomer origin, as compared to +12.01 and −5.09 cm^{-1} for the 2361.15 and 2344.08 cm^{-1} bands of the normal isotopologue. The two lowest energy predicted isomers of $(CO_2)_{10}$ are both oblate asymmetric tops with similar rotational constants. The main difference is in *A* which is smaller for isomer 10a (see Table I). Both are in satisfactory agreement with experiment, but the predicted *A* value for isomer 10a is closer. The resonant dipole model predicts the strongest band for both isomers to be the most blueshifted one and to be predominantly *c*-type. Isomer 10a, with a predicted shift of +10.43 cm^{-1}, agrees better with experiment. Agreement is not so good for the observed redshifted band at 2344.08 cm^{-1}, but the model does predict weaker *c*-type bands (not shown in Table II) for isomer 10a with shifts of −6.57 and −7.75 cm^{-1}.

F. The carbon dioxide hendecamer $(CO_2)_{11}$ and dodecamer $(CO_2)_{12}$

An even stronger *Q*-branch appears at 2361.77 cm^{-1}, just 0.6 cm^{-1} above that assigned to $(CO_2)_{10}$. It is accompanied by rather indistinct *P*- and *R*-branch structure whose spacing corresponds to an effective *B*-value of about 125 MHz, somewhat less than that of $(CO_2)_{10}$ which was about 150 MHz. This appears to be a parallel (*a*- and/or *c*-type) band of an asymmetric rotor which is heavier and more asymmetric than $(CO_2)_{10}$. Our best simulation, shown in the bottom panel of Fig. 5 together with the observed spectrum, reproduces the

TABLE VI. Molecular parameters for $(CO_2)_9$, $(CO_2)_{10}$, $(CO_2)_{11}$, $(CO_2)_{12}$, and $(CO_2)_{13}$.

	$(CO_2)_9$[a]	$(CO_2)_{10}$[b]	$(CO_2)_{11}$[c]	$(CO_2)_{12}$[d]	$(CO_2)_{13}$[e]
ν_0 / cm^{-1}	2358.6882	2361.1492 (I) 2344.0849 (II)	2361.769	2364.342	2367.7038 (I) 2368.0048 (II) 2345.0120 (III)
A'' / MHz	207	155.40	136	109	
B'' / MHz	161	144.02	114	106	92.62
C'' / MHz	125	111	97	93	90

[a]Centrifugal distortion parameters were fixed to zero. $A' - A'' = +0.40$, $B' - B'' = -0.12$, $C' - C'' = -0.15$ MHz.
[b]$A' - A'' = -0.08$ or $+0.02$, $B' - B'' = -0.09$ or $+0.01$, $C' - C'' = -0.04$ or -0.07 MHz for band I or band II, respectively.
[c]$A' - A'' = -0.06$, $B' - B'' = -0.05$, $C' - C'' = -0.04$ MHz. The ratio of intensity components for the simulation was (a:b:c) = (1.0:0:0.64). Individual rotational constants were only determined within about 5 MHz, but $(A + B)/2$ should be good to ± 2 MHz.
[d]$A' - A'' = -0.11$, $B' - B'' = -0.12$, $C' - C'' = -0.12$ MHz. The ratio of intensities for the simulation was (a:b:c) = (1.0:0.90:0.05).
[e]$B' - B'' = -0.08$ or -0.07 or 0.00, and $C' - C'' = -0.06$ or -0.04 or -0.04 MHz for band I or band II or band III, respectively. The intensity ratio for the simulation was 0.9:1.0 for band I:band II.

essential features of the band, but is less satisfactory as those of $(CO_2)_6$, $(CO_2)_7$, and $(CO_2)_{10}$. The main problem is the fuzzy character of the observed *P*- and *R*-structure, which means there is not much obvious information content. The rotational constants in the simulation agree well with predicted values for $(CO_2)_{11}$ (Tables I and VI). The simulation combines *c*- and *a*-type transitions with an intensity ratio of $c{:}a = 1{:}0.8$, and its best determined aspect is the combination $(A + B)/2 = 125$ MHz. There is a possible candidate for $(^{12}C^{18}O_2)_{11}$ centered at 2326.753 cm^{-1}, but its *P* and *R* structures are not clear. This would represent a shift of +12.70 cm^{-1} from the monomer origin, as compared to +12.63 cm^{-1} for the normal isotope. The predicted structure of $(CO_2)_{11}$ is unsymmetric, and the resonant dipole model predicts its second strongest band to be predominantly *c*-type with a shift of +10.39 cm^{-1}. This sounds good, but this predicted band also has significant *b*-type, and no *a*-type, character, in poor agreement with the observed band.

A strong and interesting feature which we assign as the *Q*-branch of $(CO_2)_{12}$ appears at 2364.34 cm^{-1}, as illustrated in Fig. 6 for two different experimental conditions. It is surrounded by periodic structure with a spacing corresponding to an effective *B*-value around 100 MHz. A simulation which is excellent for the *Q*-branch and reasonable for the rest of the band (see Fig. 3 of Ref. 28) was achieved using a combination of *a*-, *b*- and *c*-type transitions of a nearly spherical asymmetric rotor with parameters as listed in Table VI. These agree very well with those predicted for $(CO_2)_{12}$, whose structure is again unsymmetric (see Fig. 2). The resonant dipole model predicts (Table II) the second strongest band of this cluster to be strongly blueshifted (+12.14 cm^{-1}), in reasonable accord with the observed value, +15.20 cm^{-1}. The predicted intensity ratio is $a{:}b{:}c = 1.00{:}0.83{:}0.08$ as compared to that used in the simulation, $a{:}b{:}c = 1.00{:}0.95{:}0.22$.

G. The carbon dioxide tridecamer (or triskaidecamer), $(CO_2)_{13}$

The remarkable symmetric structure of $(CO_2)_{13}$ shown in Fig. 2 has been predicted in many calculations.[46,53–55] This is calculated to the most stable isomer by over 400 cm^{-1} using the M-O-M potential, and there can be little doubt that it is the "true" $(CO_2)_{13}$ structure. There is a single CO_2 monomer at the center of mass aligned along the cluster *c* axis, which is an S_6 rotation-reflection axis. This is surrounded by a cage of 12 monomers whose C atoms lie at the vertices of a slightly distorted icosahedron. There are two sets of six equivalent CO_2 monomers in the cage. The first ("equatorial") set forms a puckered ring located close to the "equatorial" plane (the plane perpendicular to the *c* axis passing through the center of mass). Three of the C atoms are slightly "above" the plane, and the alternating three are "below" the plane. The second ("polar") set of six equivalent monomers consists of two separated rings of three located above and below the equatorial plane.

The fundamental $(CO_2)_{13}$ vibrations in the CO_2 ν_3 region can be visualized as follows. One A_u mode is associated with the central monomer and gives rise to an infrared-allowed parallel band. Two further A_u modes (one for each equivalent set

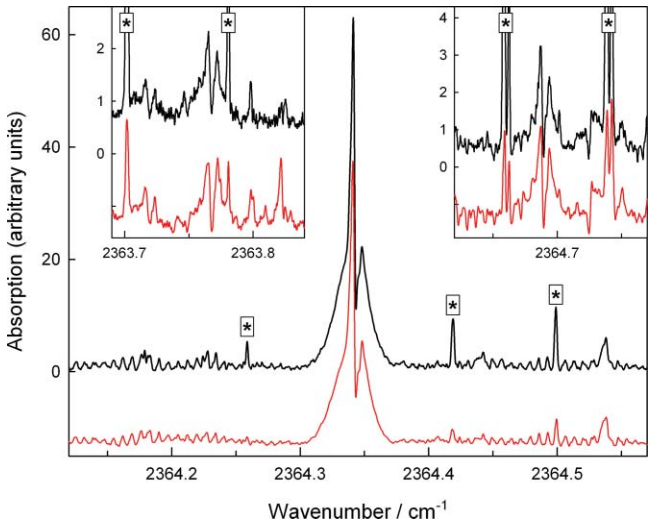

FIG. 6. Observed spectra of the band assigned to $(CO_2)_{12}$. The lower (red) trace has a larger fraction of CO_2 in the expansion gas mix. Asterisks indicate known lines due to $(CO_2)_3$ (Ref. 11). The insets show weak features (2363.77 and 2364.69 cm^{-1}) that appear to mimic the strong $(CO_2)_{12}$ *Q*-branch at 2364.34 cm^{-1} (see text).

of 6) have the "upper" three monomers in-phase with each other, the "lower" three also mutually in-phase, but with upper and lower sets are out-of-phase. Two infrared-forbidden A_g modes are associated with the in-phase vibrations of the two sets of six equivalent monomers. The remaining modes are degenerate ones, two with E_g symmetry and two with E_u symmetry. Each group of three monomers has a degenerate mode (like that of the cyclic CO_2 trimer),[7] which can either be in-phase or out-of-phase with the mirror-image group of 3, giving the total of 4 doubly degenerate modes. In reality, modes of a given symmetry are mixed and not pure as implied by these descriptions. For the resonant dipole model, the eigenvectors show that the most redshifted A_u mode (-10.98 cm^{-1}) tends to be associated with the central monomer vibration, while the middle one (-1.16 cm^{-1}) is associated with the "polar" monomers, and the blueshifted one ($+14.64$ cm^{-1}) with the central and "equatorial" ones. For E_u symmetry, the redshifted mode (-6.15 cm^{-1}) is more equatorial in character and the blueshifted one ($+5.47$ cm^{-1}) more polar, whereas the reverse is true for the E_g modes. The A_g modes are a fairly even mixtures of equatorial and polar.

Two neighboring bands near 2368 cm^{-1} with very strong Q-branches and clear P- and R-branches can be well simulated (see Fig. 3 of Ref. 28) as symmetric top parallel bands arising from a common ground state with a rotational constant very close to that predicted for $(CO_2)_{13}$. Assignment of these bands to $(CO_2)_{13}$ is supported by the fact that true symmetric tops are rare among predicted CO_2 clusters in this size range. The slight difference between the observed (92.62 MHz) and predicted (e.g., 94.8 MHz, Table I) B'' values is consistent with the other clusters observed here – the observed rotational constants are almost always 1%–4% smaller than the predicted values (Table I). This is at least partly explained by the effects of zero-point vibration (equilibrium bonds are shorter than zero-point bonds). We have now found another weaker but otherwise similar band at 2345.0 cm^{-1} whose fitted B''-value is the same to within less than 0.1 MHz, and conclude that it is also due to $(CO_2)_{13}$. The parameters used to simulate the bands are summarized in Table VI.

Since the predicted $(CO_2)_{13}$ structure is very close to being an "accidental" spherical top ($B \approx C$), it is possible that one or more of the three observed bands could be perpendicular, rather than parallel, since this distinction vanishes at the spherical limit. Testing this possibility, we found that it could be valid as long as $(B - C)$ is less than about 1 MHz (rather than 1.7 MHz as predicted), and also found that the resulting B'' and C'' values (≈92.5 and 93.5 MHz) were then slightly closer to the theoretical ones. However, these simulations did not fit the experiment quite so well.

The resonant dipole model predicts a fairly strong blueshifted (+14.64 cm) parallel band for $(CO_2)_{13}$, but we observe two such bands (+18.56 and +18.86 cm^{-1}) of almost equal strength. Of course we already know that the model is not especially reliable. But it still seems unlikely to have two fundamentals with such large shifts so close together. A possible explanation is that the two arise from an accidental Fermi-type resonance between a single "bright" blueshifted fundamental and a "dark" combination band which is the sum of one of the other fundamentals (perhaps a redshifted one) plus a low-frequency (≈20 cm^{-1}) intermolecular mode. This would help to explain the very similar appearance of these two bands. The redshifted (-4.13 cm^{-1}) band at 2345.0 cm^{-1} could then be one of the remaining A_u (or possibly E_u) fundamentals.

Support for the combination band explanation is offered by fact that combination bands are observed[10,11] for the somewhat similar $(CO_2)_3$ and $(CO_2)_6$ clusters, as noted above. Moreover, there appear to be weak "replicas" of the distinctive $(CO_2)_{12}$ Q-branch located nearby at 2363.77, 2364.69, and 2365.00 cm^{-1} (see the insets in Fig. 6). These could well be weak "background" combination bands, which acquire some intensity from the main fundamental at 2364.34 cm^{-1}. We also observe unexplained features near the $(CO_2)_7$, $(CO_2)_9$, $(CO_2)_{10}$, and $(CO_2)_{11}$ bands which could be Q-branches of background combination bands of these clusters (see Figs. 4 and 5).

III. DISCUSSION

A. Validity of the assignments

The experimental rotational constants determined here generally agree very well with calculations based on the M-O-M (Refs. 37 and 38 and SAPT-s (Ref. 30) potentials (see Table I), though we have to keep in mind that this agreement formed the basis of the assignments in the first place. As already noted, most of the experimental A, B, and C values are a bit smaller than the theoretical ones, a difference which can be ascribed in part to the effects of anharmonicity and zero-point motion which tend to make actual ground state bonds longer than equilibrium ones (and hence make rotational constants smaller). But agreement between experiment and theory does not necessarily mean that all the calculated structures are exactly correct since, for a given cluster, there may be a number of isomers which are similar in energy and which have similar rotational constants (such as isomers 10a and 10b).

Of the eight CO_2 clusters discussed here, the assignments for $(CO_2)_7$ and the two isomers of $(CO_2)_6$ are probably the most secure and those for $(CO_2)_9$ and $(CO_2)_{11}$ the least secure. It is natural that assignments become less certain as cluster size increases because the rotational structure becomes more difficult to fully resolve and also because the difference between predicted rotational parameters for successive clusters becomes smaller. What is certain is that we have a series of specific and detailed assignments, which can be directly tested by future calculations and experiments. The regularity of vibrational shifts discussed in the following subsection provides further support, especially since it was not a criterion in the original assignments.

B. Vibrational shifts

A striking feature of the assigned CO_2 cluster bands is that they show a regularly increasing blueshift with cluster size, except for the $(CO_2)_{10}$ and $(CO_2)_{13}$ bands near 2345 cm^{-1}. This is illustrated in Fig. 7, which includes the known CO_2 monomer, dimer,[5] and trimer[7,8] fundamental band origins. It has been speculated that a prominent

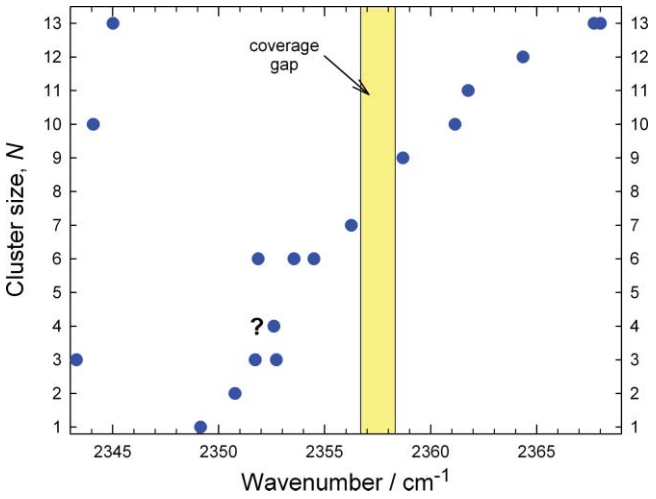

FIG. 7. Observed band origins as a function of CO_2 cluster size.

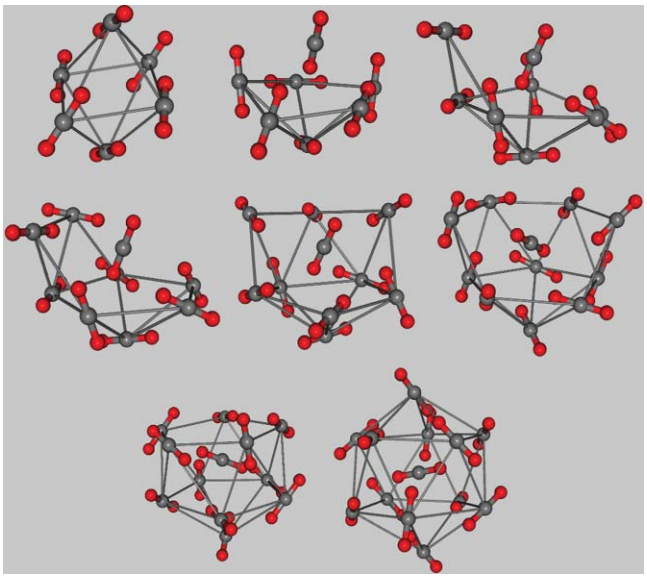

FIG. 8. Calculated structures of $(CO_2)_N$ clusters from $N = 6$ (upper left) to 13 (lower right). Thin gray nearest-neighbor C–C bonds are added to illustrate cluster growth trends.

Q-branch feature at 2352.60 cm^{-1} (labeled "Q_A") (Refs. 7, 8, and 10) might be due to $(CO_2)_4$ and this point is also included in Fig. 7 with a question mark. From this plot, it appears that a band of $(CO_2)_8$ is expected near 2357.5 cm^{-1}, but we have not been able to investigate this range for $^{12}C^{16}O_2$ due to a gap in laser coverage. In the case of $^{12}C^{18}O_2$, there are sharp Q-branches at 2321.945, 2321.955, and 2321.964 cm^{-1} with relative peak heights of 1.0:0.7:0.3. One or more of these could be due to $(CO_2)_8$, but the accompanying P- and R-branches were not strong or structured enough to be analyzed. The strongest one represents a shift of +7.90 cm^{-1} which would put the corresponding band for the $^{12}C^{16}O_2$ tetramer at 2357.04 cm^{-1}, within the gap region. It also seems that a band of $(CO_2)_5$ should appear around 2353 cm^{-1}, and there are possible candidate Q-branches at 2353.26, 2353.45, and 2353.75 cm^{-1} (these are visible in Fig. 2(a) of Ref. 28).

We observe one to three bands per cluster, but of course the larger clusters have many more allowed fundamental bands in the CO_2 ν_3 region. Figure 7 seems to indicate that the bands we actually observe, which are presumably the stronger or strongest ones, tend to blueshift increasingly from about 2350 to 2370 cm^{-1} with a slope of about +1.5 cm^{-1} per added CO_2 going from CO_2 to $(CO_2)_{13}$. The tendency of the CO_2 ν_3 vibration to blueshift for medium or large clusters is already known from low-resolution studies.[22,29] As we have seen it is also predicted by the resonant dipole model, though with a smaller magnitude than observed here (see Fig. 1 of Ref. 28). It is important to recognize that bands of larger clusters which happen to lie close to the monomer band origin (2349.14 cm^{-1}) are inherently difficult to detect and recognize because of the presence of stronger bands of smaller clusters (dimer, trimer, etc.). So there is a selection effect favoring bands with larger shifts which occur in clear regions of the spectrum. Another selection effect is that symmetric clusters (and unsymmetric ones with rotational constants closer to the prolate or oblate limit) are more likely to be assigned because their spectra tend to be more easily recognized and stronger (less spread out).

C. Cluster structures

Acknowledging that the present results do not contain much structural information, we have not said much yet about the detailed cluster structures except for $(CO_2)_6$ and $(CO_2)_{13}$. However, since the results do support the general validity of the structures based on the M-O-M and SAPT-s potentials, it is interesting to examine their evolution in the range from $N = 6$ to 13, focusing on C atom positions rather than individual monomer orientations.

The calculated structures are pictured in Fig. 8, proceeding from $(CO_2)_6$ in the upper left corner to $(CO_2)_{13}$ in the lower right. Certain C–C bonds are added to help visualize the growth trends. The two symmetric isomers of $(CO_2)_6$ have already been described. $(CO_2)_7$ is approximately a pentagonal ring of CO_2 monomers with single monomers located "above" and "below" the (roughly) planar ring. This is more closely related to the S_4 isomer of $(CO_2)_6$ than to the lower energy S_6 isomer, since it can be formed by adding one more CO_2 to the ring of four equivalent monomers in the S_4 isomer. We can also think of $(CO_2)_7$ as being a shallow "cup" (formed by the pentagon and bottom monomers) holding a single "interior" CO_2 (the top monomer). From $N = 8$ to 12, a second pentagonal ring forms "above" the first one, steadily enclosing the interior monomer in a deeper cup. Finally, in $(CO_2)_{13}$ a top monomer is added to the cup and the interior monomer is completely enclosed. But a new symmetry emerges: rather than imagining $(CO_2)_{13}$ to be approximately composed of an interior monomer enclosed by two pentagonal rings plus top and bottom monomers (1-5-5-1 ring structure), we find that it is precisely composed of the interior monomer enclosed by a staggered ring of six equivalent monomers plus two equivalent rings of three monomers (3-6-3 ring structure), as described above in Sec. II G and Fig. 2. This underlying 3-6-3 ring motif is sometimes evident for clusters in the $N = 8$–12 range.

IV. CONCLUSIONS

The predicted structures and resulting rotational constants for carbon dioxide clusters in the range $N = 5$–13 calculated assuming pairwise additivity show good agreement using two intermolecular potential functions obtained from very different sources, M-O-M (Refs. 37 and 38) and SAPT-s.[30] With the help of these predictions, we assign 13 specific infrared bands in the CO_2 ν_3 fundamental region ($\approx$2350 cm^{-1}) to clusters with $N = 6$, 7, 9, 10, 11, 12, and 13. Three of these bands are also observed for $^{12}C^{18}O_2$ clusters. The clusters are produced in a pulsed supersonic expansion using a slit jet source and the spectra are recorded by direct absorption using a tuneable diode laser probe. Two isomers are observed for $(CO_2)_6$, both of which are oblate symmetric tops. The lowest energy form has S_6 symmetry and the other has S_4 symmetry. $(CO_2)_{13}$ is also an S_6 oblate symmetric top, but the remaining clusters are asymmetric tops with no symmetry elements (C_1 point group). The effective rotational constants obtained by fitting or simulating the observed bands are generally 1%–4% smaller than the equilibrium constants predicted by the intermolecular potentials, an effect which is at least partly due to zero point motion. The stronger observed bands show a progressive vibrational blueshift with increasing cluster size. Such shifts are similar to, but significantly larger in magnitude than, those predicted by the resonant dipole-dipole interaction model. These are the largest such molecular clusters to be assigned to specific infrared bands with at least partial rotational resolution. The results provide precise benchmarks for future theoretical calculations. They should also enable the growth of different sized clusters to be monitored dynamically in various supersonic jet (and other) environments. As well, the sharp and strong nature of most of the observed Q-branches may facilitate new experiments in which energy could be selectively deposited into clusters of a particular size using a tuneable pump laser.

ACKNOWLEDGMENTS

We thank L. Murdock for technical assistance. Many of our results were greatly facilitated by the use of PGOPHER, and we are pleased to acknowledge C. M. Western for helpful advice and program updates. We gratefully acknowledge the financial support of the Natural Sciences and Engineering Research Council of Canada.

[1] R. E. Miller and R. O Watts, Chem. Phys. Lett. **105**, 409 (1984).
[2] K. W. Jucks, Z. S. Huang, D. Dayton, R. E. Miller, and W. J. Lafferty, J. Chem. Phys. **86**, 4341 (1987).
[3] K. W. Jucks, Z. S. Huang, R. E. Miller, G. T. Fraser, A. S. Pine, and W. J. Lafferty, J. Chem. Phys. **88**, 2185 (1988).
[4] A. S. Pine and G. T. Fraser, J. Chem. Phys. **89**, 100 (1988).
[5] M. A. Walsh, T. H. England, T. R. Dyke, and B. J. Howard, Chem. Phys. Lett. **142**, 265 (1987).
[6] G. T. Fraser, A. S. Pine, W. J. Lafferty, and R. E. Miller, J. Chem. Phys. **87**, 1502 (1987).
[7] M. J. Weida, J. M. Sperhac, and D. J. Nesbitt, J. Chem. Phys. **103**, 7685 (1995).
[8] M. J. Weida and D. J. Nesbitt, J. Chem. Phys. **105**, 10210 (1996).
[9] T. Konno and Y. Ozaki, Chem. Phys. Lett. **394**, 198 (2004).
[10] M. Dehghany, A. R. W. McKellar, M. Afshari, and N. Moazzen-Ahmadi, Mol. Phys. **108**, 2095 (2010).
[11] M. Dehghany, M. Afshari, N. Moazzen-Ahmadi, and A. R. W. McKellar, J. Chem. Phys. **128**, 064308 (2008).
[12] L. Mannik, J. C. Stryland, and H. L. Welsh, Can. J. Phys. **49**, 3056 (1971).
[13] Y. I. Baranov and A. A. Vigasin, J. Mol. Spectrosc. **193**, 319 (1999).
[14] A. A. Vigasin, J. Mol. Spectrosc. **200**, 89 (2000).
[15] A. A. Vigasin, F. Huisken, A. I. Pavlyuchko, L. Ramonat, and E. G. Tarakanova, J. Mol. Spectrosc. **209**, 81 (2001).
[16] A. A. Vigasin, Y. I. Baranov, and G. V. Chlenova, J. Mol. Spectrosc. **213**, 51 (2002).
[17] Y. I. Baranov, W. J. Lafferty, G. T. Fraser, and A. A. Vigasin, J. Mol. Spectrosc. **218**, 260 (2003).
[18] G. A. Pubanz, M. Maroncelli, and J. W. Nibler, Chem. Phys. Lett. **120**, 3 (1985).
[19] F. Huisken, L. Ramonat, J. Santos, V. V. Smirnov, O. M. Stelmakh, and A. A. Vigasin, J. Mol. Struct. **410–411**, 47 (1997).
[20] A. Ramos, J. M. Fernández, G. Tejeda, and S. Montero, Phys. Rev. A **72**, 053204 (2005).
[21] T. E. Gough, R. E. Miller, and G. Scoles, J. Phys. Chem. **85**, 4041 (1981).
[22] J. A. Barnes and T. E. Gough, J. Chem. Phys. **86**, 6012 (1987).
[23] J. A. Barnes, T. E. Gough, and M. Stoer, J. Chem. Phys. **95**, 4840 (1991).
[24] R. Disselkamp and G. E. Ewing, J. Chem. Phys. **99**, 2439 (1993).
[25] S. Bauerecker, M. Taraschewski, C. Weitkamp, and H. K. Cammenga, Rev. Sci. Instrum. **72**, 3946 (2001).
[26] G. Torchet, M. F. de Feraudy, A. Boutin, and A. H. Fuchs, J. Chem. Phys. **105**, 3671 (1996).
[27] A. Bonnamy, R. Georges, A. Benidar, J. Boissoles, A. Canosa, and B. R. Rowe, J. Chem. Phys. **118**, 3612 (2003).
[28] J. Norooz Oliaee, M. Dehghany, N. Moazzen-Ahmadi, and A. R. W. McKellar, Phys. Chem. Chem. Phys. **13**, 1297 (2011).
[29] A. Bonnamy, R. Georges, E. Hugo, and R. Signorell, Phys. Chem. Chem. Phys. **7**, 963 (2005).
[30] R. Bukowski, J. Sadlej, B. Jeziorski, P. Jankowski, K. Szalewicz, S. A. Kucharski, H. L. Williams, and B. M. Rice, J. Chem. Phys. **110**, 3785 (1999).
[31] S. Tsuzuki, W. Klopper, and H. P. Lüthi, J. Chem. Phys. **111**, 3846 (1999).
[32] S. Bock, E. Bich, and E. Vogel, Chem. Phys. **257**, 147 (2000).
[33] M. T. Oakley and R. J. Wheatley, J. Chem. Phys. **130**, 034110 (2009).
[34] G. Cardini, V. Schettino, and M. L. Klein, J. Chem. Phys. **90**, 4441 (1989).
[35] Z. Zhang and Z. Duan, J. Chem. Phys. **122**, 214507 (2005).
[36] T. Merker, C. Engin, J. Vrabec, and H. Hasse, J. Chem. Phys. **132**, 234512 (2010).
[37] C. S. Murthy, K. Singer, and I. R. McDonald, Mol. Phys. **44**, 135 (1981).
[38] C. S. Murthy, S. F. O'Shea, and I. R. McDonald, Mol. Phys. **50**, 531 (1983).
[39] M. Dehghany, M. Afshari, Z. Abusara, C. Van Eck, and N. Moazzen-Ahmadi, J. Mol. Spectrosc. **247**, 123 (2008).
[40] M. Dehghany, M. Afshari, N. Moazzen-Ahmadi, and A. R. W. McKellar, Phys. Chem. Chem. Phys. **10**, 1658 (2008).
[41] M. Dehghany, M. Afshari, R. I. Thompson, N. Moazzen-Ahmadi, and A. R. W. McKellar, J. Mol. Spectrosc. **252**, 1 (2008).
[42] M. Dehghany, M. Afshari, J. Norooz Oliaee, N. Moazzen-Ahmadi, and A. R. W. McKellar, Chem. Phys. Lett. **473**, 26 (2009).
[43] PGOPHER, a program for simulating rotational structure, C. M. Western, University of Bristol, U.K; see http://pgopher.chm.bris.ac.uk.
[44] M. J. Weida, J. M. Sperhac, D. J. Nesbitt, and J. M. Hutson, J. Chem. Phys. **101**, 8351 (1994).
[45] A. R. W. McKellar, J. Chem. Phys. **125**, 114310 (2006).
[46] H. Takeuchi, J. Phys. Chem. A **112**, 7492 (2008).
[47] W. H. Press, S. A. Reukolsky, W. T. Vetterling, and B. P. Flannery, *Numerical Recipes in FORTRAN*, 2nd ed. (Cambridge University Press, Cambridge, England, 1992).
[48] J. Geraedts, M. Waayer, S. Stolte, and J. Reuss, Faraday Discuss. Chem. Soc. **73**, 375 (1982).
[49] R. Signorell, J. Chem. Phys. **118**, 2707 (2003).
[50] I. V. Boychenko and H. Huber, J. Chem. Phys. **124**, 014305 (2006).
[51] V. M. Devi, B. Fridovich, G. D. Jones, and D. G. S. Snyder, J. Mol. Spectrosc. **105**, 61 (1984).
[52] K. V. J. Jose and S. R. Gadre, J. Chem. Phys. **128**, 124310 (2008).
[53] H. Liu and K. D. Jordan, J. Phys. Chem. A **107**, 5703 (2003).
[54] J.-B. Maillet, A. Boutin, S. Buttefay, F. Calvo, and A. H. Fuchs, J. Chem. Phys. **109**, 329 (1998).
[55] R. D. Etters, K. Flurchick, R. P. Pan, and V. Chandrasekharan, J. Chem. Phys. **75**, 929 (1981).